Geomechanics and Engineering, *Vol. 24, No. 6 (2021) 531-543*
DOI: https://doi.org/10.12989/gae.2021.24.6.531

Effects of freezing and thawing on retaining wall with changes in groundwater level

Garam Kim, Incheol Kim, Tae Sup Yun and Junhwan Lee*

School of Civil and Environmental Engineering, Yonsei University, 50, Yonsei-ro, Seodaemun-gu, Seoul 03722, Republic of Korea

(Received August 25, 2020, Revised February 9, 2021, Accepted March 16, 2021)

Abstract. Freezing and thawing of pore water within backfill can affect the stability of retaining wall as the phase change of pore water causes changes in the mechanical characteristics of backfill material. In this study, the effects of freezing and thawing on the mechanical performance of retaining wall with granular backfill were investigated for various temperature and groundwater level (GWL) conditions. The thermal and mechanical finite element analyses were performed by assigning the coefficient of lateral earth pressure according to phase change of soil for at-rest, active and passive stress states. For the at-rest condition, the mobilized lateral stress and overturning moment changed markedly during freezing and thawing. Active-state displacements for the thawed condition were larger than for the unfrozen condition whereas the effect of freezing and thawing was small for the passive condition. GWL affected significantly the lateral force and overturning moment (M_o) acting on the wall during freezing and thawing, indicating that the reduction of safety margin and wall collapse due to freezing and thawing can occur in sudden, unexpected patterns. The beneficial effect of an insulation layer between the retaining wall and the backfill in reducing the heat conduction from the wall face was also investigated and presented.

Keywords: freezing, thawing; retaining wall; temperature; groundwater level; lateral stress; overturning moment

1. Introduction

Freezing and thawing of soil are commonly observed in regions where the temperature fluctuates periodically with season. The effects of freezing and thawing on soils have been extensively studied, mainly regarding changes in the mechanical properties and volume-change behavior (Chamberlain and Gow 1979, Qi *et al*. 2006, Lee *et al*. 2016, Liu *et al*. 2016). According to Qi *et al*. (2006), the void ratios of dense and loose soils increase and decrease, respectively, with freezing-thawing cycle while the permeability increases due to the freezing and melting process of pore water (Eigenbrod 1996, Zhang *et al*. 2014, Jin *et al*. 2019). The volume-change behavior of soil during freezing and thawing are closely related to frost heave and thaw consolidation. Through freezing and thawing, the particle configuration and microstructure alter because of changes in the pore water phase and overall volume. As fine-grained soil is influenced more by moisture with higher frost susceptibility, the majority of freezing and thawing–related investigations were focused on fine-grained soils. Some cases of the effects of freezing and thawing for coarse-grained granular soils were also reported (Zhang *et al*. 2014, Lee *et al*. 2016, Liu *et al*. 2016, Kim *et al*. 2021). Liu *et al*. (2016) found that the internal friction angle of silty sands decreased and increased with increasing number of freezing and thawing cycle. Lee *et al*. (2016) and Kim *et al*. (2021) observed an increase in volume and lateral earth pressure in sand after freezing and thawing.

Retaining walls are sensitive to freezing and thawing as the walls and backfills have air-exposed exterior surfaces often with moisture or groundwater. The effects of moisture or groundwater on retaining walls have been addressed and investigated for the stability associated with mobilized pore-water pressure, reductions in the effective strength, and rainfall infiltration through backfill materials (Blake *et al*. 2003, Yoo and Jung 2006). With regard to the freezing and thawing problem, the target issues were frost heave and thaw consolidation of fine-grained backfill materials, which represent the pre-failure characteristics of volume change behavior and compressibility (Michałowski and Zhu 2006, Zhang 2014).

For coarse-grained soils, it was presented that the internal friction angle decreased during freezing and thawing, different from that clays (Wang *et al*. 2007, Liu *et al*. 2016). According to Zhang *et al*. (2014), the pore water pressure in coarse-grained soils decreased and increased during freezing and thawing, respectively, which is affected by the degree of saturation. Changes in volume and the mechanical properties of sands under freezing and thawing were more pronounced for fully saturated condition (Lee *et al*. 2016, Kim *et al*. 2021). The changes were negligible for partially saturated or unsaturated conditions (Kim *et al*. 2021). This indicates that the groundwater level in the backfill of retaining wall should be considered for the freezing and thawing problems. In addition, the freezing temperature can also be a factor for the effect of freezing and thawing on backfill as the backfill often exposed to air with variable temperature (Zhang 2014).

*Corresponding author, Professor, Ph.D.
E-mail: junlee@yonsei.ac.kr

ISSN: 2005-307X (Print), 2092-6219 (Online)

For the stability of retaining wall, the lateral earth pressure acting on the wall is a key component, which varies with stress history, material constitution and density conditions (Brooker and Ireland 1965, Clough and Duncan 1971, Bentler and Labuz 2006, Lee 2019). It was recently reported that the stress states of moist granular soils are largely affected by temperature and freezing-thawing process (Yao *et al*. 2014, Lee *et al*. 2016). According to Lee *et al*. (2016), the lateral earth pressure of granular soils increases through the process of freezing and thawing, indicating a higher coefficient of lateral earth pressure. This means that both thermal and mechanical aspects need to be included for the stability of retaining walls subject to freezing and thawing, which may require certain coupled or correlated procedure. Most of the previous analyses were targeted at wall movements due to frost heave and thaw consolidation for retaining walls placed in frost-susceptible soils (Michałowski and Zhu 2006, Zhang 2014). The stability-related issues with the effects of freezing and thawing on retaining walls have not been specifically addressed in detail.

In the present study, the effects of freezing and thawing on the stability of the retaining walls were investigated, focusing on changes in the stress state, consequence to the overall stability and the influence of groundwater level (GWL). For this purpose, the thermal and subsequent mechanical finite element (FE) analyses were performed interactively for various environmental and soil conditions including changes in external air temperature, freezing-thawing duration and GWL location within backfill. All possible stress states of at-rest, active, and passive conditions were considered and taken into the analysis. The effectiveness of thermal insulation layer on wall face was investigated as well.

2. Thermal and mechanical characteristics of soil

2.1 Heat transfer mechanism

The characteristics of soil heat transfer are closely related to the composition of the soil, given by the particle type, water and air void. The main modes of heat transfer mechanism within soil are conduction, convection, and radiation, as described in Fig. 1. For soil, heat transfer by conduction plays an important role, whereas convection and radiation indicate negligible effects (Milly 1984, Jame and Norum 1980). Different types of conduction mechanisms exist within soil through particles, pore fluids and their contact interfaces, as shown in Fig. 1, all of which contribute to the heat transfer within the soil.

Key thermal properties of soil that control the heat-transfer mechanism are thermal conductivity (k), specific heat (C), and latent heat (L). These properties are also important for the phase-change behavior in soil, which is related to the amount of thermal energy required for a change between the unfrozen and frozen states. (Andersland and Anderson 1978, Côté and Konrad 2005, Yun and Santamarina 2008). Water usually requires less thermal energy for phase change than soil particles or air. This means that the heat-transfer behavior of soil and the required thermal energy will differ depending on the water content and location of groundwater level (GWL).

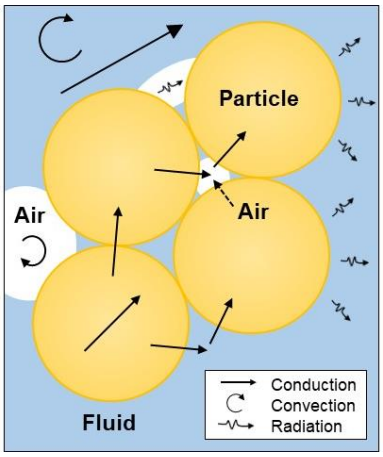

Fig. 1 Heat transfer mechanism in soils

The conduction-mode heat transfer in soil is affected by many factors such as mineralogy, particle size, applied pressure, density, and water content (Farouki 1981, Côté and Konrad 2005, Yun and Santamarina 2008). The volume fractions of water and ice within soil voids, in particular, exert significant influences on the thermal conductivity (k) of soil. Côté and Konrad (2005) proposed a generalized relationship for the thermal conductivity as a function of the degree of saturation, given as follows:

$$k_r = \frac{k - k_{dry}}{k_{sat} - k_{dry}} = \frac{\kappa S_r}{1 + (\kappa - 1) S_r} \quad (1)$$

where k_r = normalized thermal conductivity of soil; k_{sat} = thermal conductivity of saturated soil; k_{dry} = thermal conductivity of dry soil; S_r = degree of saturation; and κ = correlation parameter (3.55 and 0.95 for the unfrozen and frozen states, respectively). The values of k_r are 0 and 1 for the dry and saturated conditions, respectively.

The specific heat of soil (C) represents the amount of heat required to raise or lower the soil temperature. Water has higher specific heat than soil minerals, and the contribution of air to the specific heat of soil is negligible. The latent heat (L) corresponds to the amount of thermal energy required for a phase change during freezing and thawing. Water releases and absorbs energy during the phase change and thus controls the overall latent heat of soil. The thermal energy released or absorbed during a phase change in the soil–water mixture indicates a latent heat, as described in Fig. 2. Note that Fig. 2 represents the effect of the latent heat for coarse-grained soils while the temperature range where the phase change occurs can be larger for fine-grained soils. The thermal properties of k, C, and L described herein all are necessary for the thermal analysis of soil, and will be introduced into the thermal analysis of the retaining walls in this study.

2.2 Effects of freezing and thawing on mechanical properties of soil

As soil is composed of particles, voids and water, the

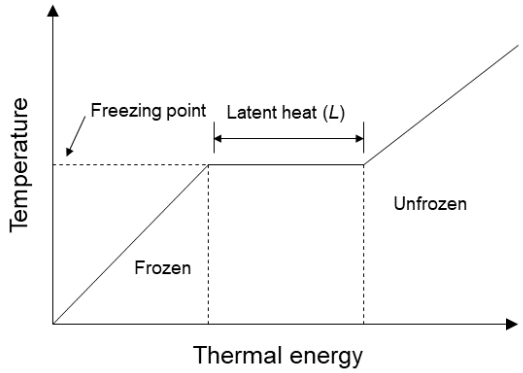

Fig. 2 Latent heat for granular soil-water mixture system

mechanical properties of soil change with freezing and thawing due to the phase and volume change behaviors of the pore water within voids (Chamberlain and Gow 1979, Zhang *et al*. 2014, Tang *et al*. 2020). The freezing of water within voids induces cementation of soil particles, providing a bonding effect with reduced compressibility and an increase in the total volume. According to Chamberlain and Gow (1979), the formation of ice lenses within soil causes negative pore pressure with increase in the effective stress during the freezing process. On thawing, the volume of soil decreases due to the melting of ice and the rearrangement of soil particles. While the void ratio tends to decrease after freezing and thawing, the permeability increases because shrinkage cracks provide flow paths for pore fluid by melting ice lenses (Chamberlain and Gow 1979, Eigenbrod 1996).

Consolidation and strength are also affected by freezing and thawing. As the number of freezing-thawing cycle increases, the coefficient of consolidation increases due to micro-fissuring and enlargement of pores within soil (Eigenbrod 1996, Paudel and Wang 2010). When the soil structure is damaged, and large pores are formed from the melting of ice within the voids, the bonding effect disappears and the stress-strain curve becomes more or less round, without clear peaks (Graham and Au 1985, Leroueil *et al*. 1991, Liu *et al*. 2016).

Yao *et al*. (2014) conducted triaxial tests for frozen soil and reported that the coefficient of the at-rest lateral earth pressure (K_0) for frozen soil decreased with decreasing temperature due to the enhanced cementing effect between soil particles and ice. The tests were conducted under an undrained condition using silty clay and coarse sand. The test results indicated that K_0 varied with water content and increased nonlinearly with increasing load level because of the crushing of the soil particles in the frozen condition.

Lee *et al*. (2016) investigated the values of K_0 for various granular materials under the unfrozen, frozen, and thawed conditions. It was found that the values of K_0 changed and were different for the unfrozen, frozen, and thawed conditions. The changes in K_0 were affected by the stress state, soil condition, relative density, confining stress, and inherent material constitution such as silt content. K_0 decreased during freezing and increased after thawing, resulting in a higher value than for the unfrozen condition.

The values of K_0 for the unfrozen, frozen, and thawed conditions reported in Lee *et al*. (2016) are shown in Fig. 3. The changes in K_0 value shown in Fig. 3 are the results from the experimental tests conducted for coarse-grained soils. K_0 decreased by up to 86% and increased by up to 74% for the frozen and thawed conditions, respectively, within a range of applied load from 16 to 160 kPa. It was also observed that the higher the degree of saturation, the greater the values of K_0 for the thawed condition. This indicates that, when groundwater or a fully saturated condition exists within backfill behind retaining wall, the freezing and thawing process itself can cause certain changes in the stability and safety margin even if there is no additional increase of external load.

3. Thermal and mechanical analysis of retaining wall

3.1 Description of analysis

Thermal and mechanical FE analyses were performed to investigate the effects of freezing and thawing on the mechanical behavior and overall stability of retaining walls. Various cases of external air temperature and GWL within backfill were considered in the analyses. The commercial FE program ABAQUS was used for thermal and subsequent mechanical analyses. For the thermal analysis, the following energy conservation equation was solved through the FE procedure to obtain the heat transfer, the thermal changes within backfill, and the spatial propagation with time:

$$C_v \frac{\partial T}{\partial t} - \nabla(k_m \nabla T) - L\rho_i \frac{\partial \theta_i}{\partial t} = 0 \qquad (2)$$

where C_v = volumetric heat capacity; k_m = heat conductivity; L = latent heat per unit mass; θ_i = volumetric fraction of ice content; ρ_i = density of ice; T = temperature; and t = time.

Once the FE model of the retaining wall and backfill was prepared, the thermal and mechanical FE analyses were conducted in sequence. The thermal FE analysis was performed for given initial temperature and GWL conditions. The durations of freezing and thawing were both set to 90 days, which was assumed sufficiently long to attain fully frozen and thawed conditions. Freezing and thawing zones within the backfill were then identified for each temperature and GWL conditions, and were incorporated into the mechanical FE-analysis step. The geostatic stress condition was assigned within the identified thermal zones with values of K_0 corresponding to the unfrozen, frozen, and thawed conditions, to consider the changes in the stress states due to the freezing-thawing process.

Backfill was assumed as coarse-grained soil with properties given in Table 1. The soil properties in Table 1 were the same as those given in Lee *et al*. (2016), where the values of K_0 for frozen and thawed condition were tested and presented. The relative density (D_R) of the backfill was 80%, adopted considering the typical compacted condition of backfill. The Mohr-Coulomb model was used to simulate the mechanical behavior of soil in the FE analysis. The

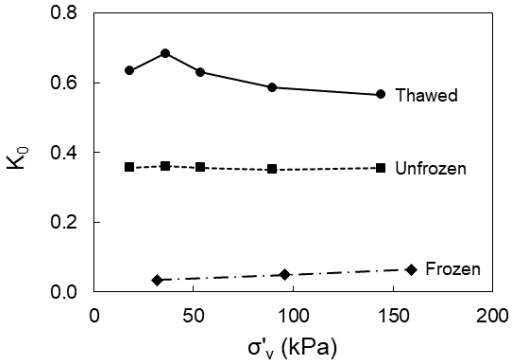

Fig. 3 Values of K_0 for unfrozen, frozen, and thawed soil conditions

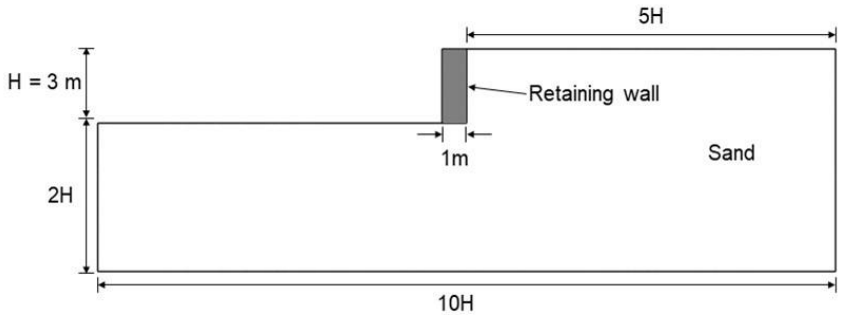

(a)

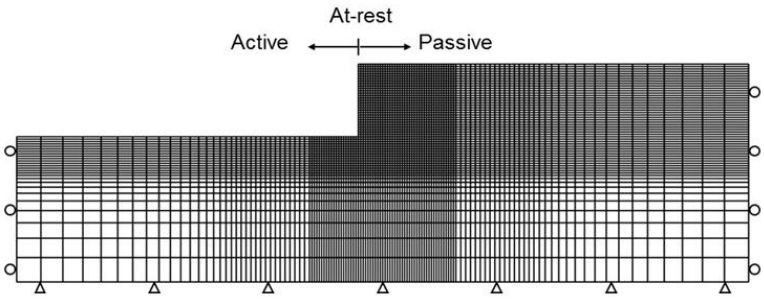

(b)

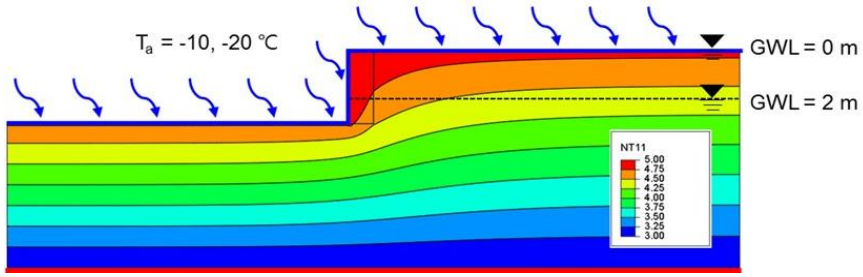

(c)

Fig. 4 FE analysis of retaining wall: (a) wall configuration, (b) finite element mesh and (c) initial temperature distribution

values of K_0 of backfill for unfrozen, frozen, and thawed conditions were equal to 0.36, 0.05, and 0.62, respectively, as given in Lee *et al.* (2016). When the geostatic equilibrium condition was achieved, the stress analysis was performed. At-rest, active, and passive stress states were all considered in the FE analyses by imposing wall displacement boundary conditions for each case.

3.2 FE modeling and analysis condition

The geometry of the retaining wall and backfill considered in the FE analysis is shown in Fig. 4(a). The retaining wall was a simple rectangular shape without base or shear key, in order to focus on the effect of freezing and thawing on the lateral earth pressure and resistance as well as on the mobilized distributions during the active and passive stress states. The retaining wall was 3-m high with a thickness of 1.0 m and assumed to be linear elastic. The model is 10 times wider laterally and 3 times longer vertically than the wall height (H). Fig. 4(b) shows the FE model prepared in this study. A fine mesh was assigned

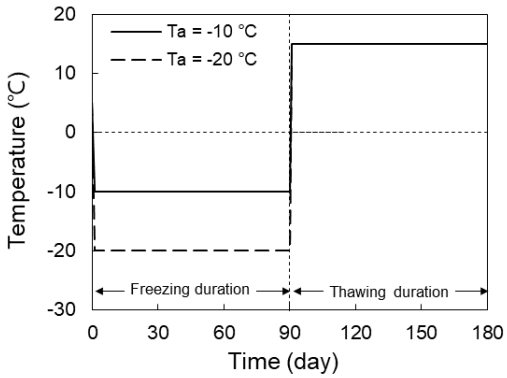

Fig. 5 Thermal boundary condition of exposed surface during freezing and thawing

Table 1 Properties of soil in mechanical FE analysis

Soil classification (USCS)	SP
Specific gravity (G_s)	2.65
Mean grain size (d_{50})	0.525 mm
Elastic modulus (E)	60 MPa
Peak friction angle (D_R = 80%) (ϕ'_p)	39.8°
Critical state friction angle (ϕ'_c)	36.4°

Table 2 Properties of soil in thermal FE analysis

Soil type	Sand (D_R = 80%)
Unit weight (γ)	15.29 kN/m^3 (dry soil)
	19.32 kN/m^3 (saturated soil)
Thermal conductivity (k)	5.77 W/m·K (soil particle)
	0.24 W/m·K (dry soil)
	2.42 W/m·K (saturated unfrozen soil)
	3.91 W/m·K (saturated frozen soil)
Specific heat capacity (C)	1532.6 J/kg·K (unfrozen soil)
	1065.6 J/kg·K (frozen soil)
Latent heat (L)	135440 J/kg

near the wall to capture the changes in temperature and stress in more detail. A fixed boundary condition was assigned at the bottom, while laterally constrained conditions were set along the vertical boundaries of the model.

Various temperatures and GWLs were considered in the FE analyses as these factors are closely related to the heat transfer and freezing-thawing behavior of the backfill. Fig. 4(c) shows the initial distribution of the internal temperature within the backfill for given input external air temperature (T_a) and GWL. The distribution of initial temperature within the backfill was set based on the previous studies of Zhang (2014) and Babaei (2016). According to Zhang (2014), the temperature becomes nearly constant around 3℃ below the depth of 7 m and Babaei (2016) considered the initial temperature range of 3℃ and 6℃ from the bottom to the exposed soil surface. The initial temperature distribution in this study was set equal to 5℃ on the ground surface and 3℃ on the bottom of FE model. Fig. 5 shows the variation of T_a with time during the freezing and thawing durations, which were set along the ground surfaces and the exposed retaining wall surface as thermal boundary conditions. The freezing and thawing of 90 days duration were assumed as a typical duration to consider the seasonal variation of temperature (Michałowski and Zhu 2006, Zhang 2014). However, it should also be noted that actual freezing and thawing durations would change depending on the location of target region. Two initial T_as of −10°C and −20℃ were adopted during freezing, while 15℃ was set for the thawing duration. Two cases of GWL were adopted at depths of 0 and 2.0 m from the backfill surface. The GWL at 0 m represented the GWL at the top surface and the fully saturated backfill condition, which could happen if the drainage holes of retaining wall were clogged or filled with impermeable frozen materials.

The soil above the GWL was maintained dry without phase change behavior. The basic thermal properties of the backfill material used in the FE analyses are given in Table 2. The values of thermal conductivity (k) and specific heat capacity (C) for each soil condition were obtained using Eq. (1) by Côté and Konrad (2005) and Andersland and Ladanyi (2004), respectively. The thermal conductivity and specific heat capacity of the concrete retaining wall were 1.2 W/m·K and 970 J/kg·K, respectively (Zhang 2014). The interface thermal characteristic between the retaining wall and backfill is usually defined by gap conductance. In this study, the interface thermal conductance was assumed the same as the thermal conductivity of the backfill for simplicity (Saggu and Chakraborty 2017).

The thermal behavior of retaining wall is influenced by various factors including heat transfer, formation of ice lens with water capillary migration, volume change of soil, and wall stiffness (Andersland and Ladanyi 2004, Zhang *et al.* 2014). If the capillary migration during the phase change of water is considered, changes in the pore water and effective stresses would also take place and affect the calculated results (Chamberlatin and Gow 1979, Eigenbrod *et al.* 1996). The FE analyses in this study were focused on the effects of freezing and thawing of backfill on the lateral earth pressure along the wall, and the heat transfer analysis was performed focusing on the heat conduction within backfill. Other possible influence factors, such as frost heave, thaw settlement, water capillary migration, and convection during freezing and thawing, were not specifically considered in the analyses.

3.3 Comparison

A case example was selected from the literature and introduced to compare with the results from the thermal analysis in this study. The full validation of the analysis would require field test cases with measured mechanical behavior of retaining wall associated with changes in temperature. As such case was hardly found from the literature, a case with the temperature distribution within the backfill of retaining wall was obtained and adopted in the comparison. This would provide the minimum level of necessary validation for the temperature distribution within a backfill, which was the key component for investigating

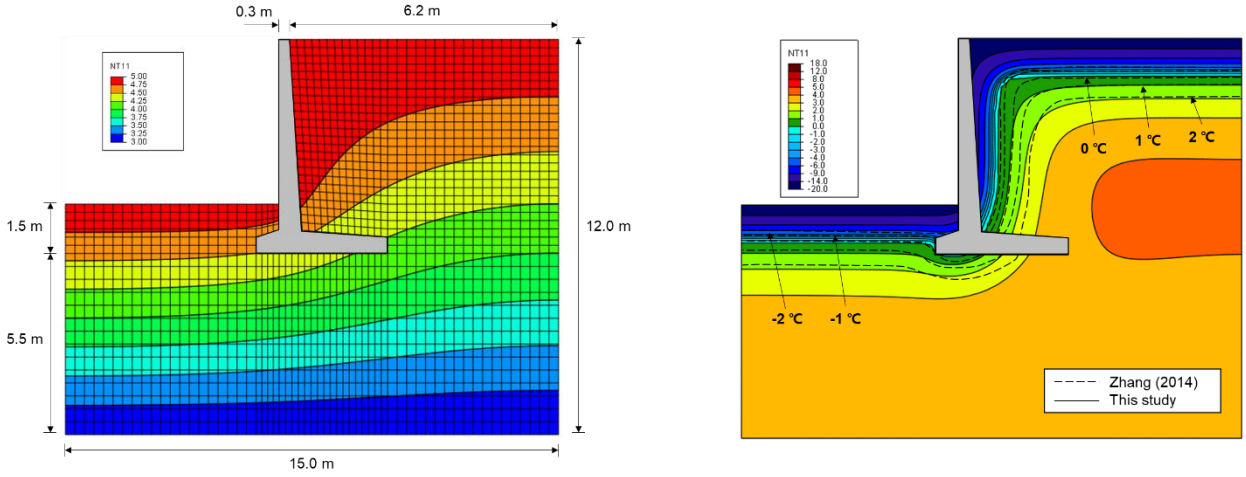

(a) (b)

Fig. 6 Comparison of temperature distributions for retaining-wall system: (a) initial temperature distribution and (b) isotherms

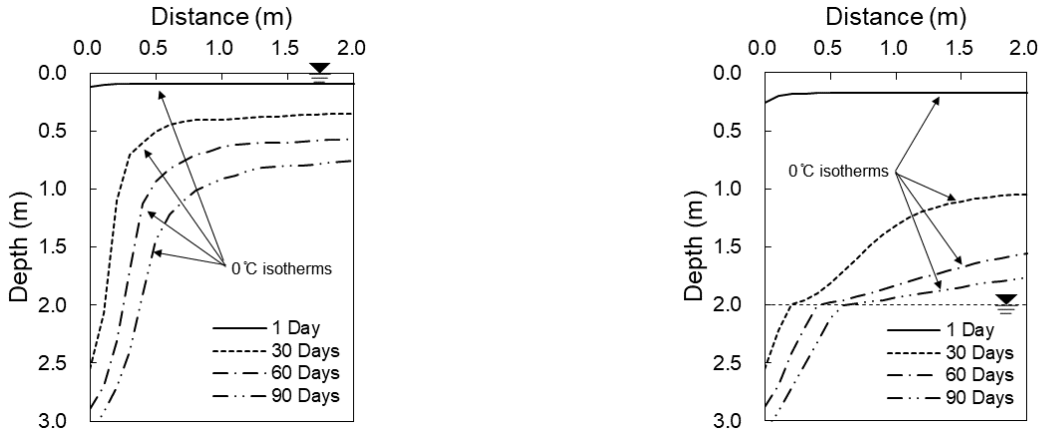

(a) (b)

Fig. 7 0℃ isotherm profiles for (a) GWL = 0 m and (b) GWL = 2 m

the mechanical behavior for retaining wall subjected to freezing and thawing. The selected case example was the thermal analysis of the retaining wall reported in Zhang (2014). The retaining wall is a cantilever type with the height and base width of 6.5 and 4.0 m, respectively, embedded 1.5 m below the ground surface. The range of initial temperature distribution within the backfill was 3℃ to 5℃ from the bottom to the exposed surface, respectively, as shown in Fig. 6(a). The external air temperature was set to vary linearly from 5°C to −20℃ for 80 days and was imposed along the external surface of the retaining wall, the backfill top surface, and the lower ground. All other thermal properties of the soil and the retaining wall used in the analysis were the same as those given in Zhang (2014).

Fig. 6(b) shows the distributions of internal temperature and isotherm contours within the backfill, obtained from this study. The results obtained by Zhang (2014) were also included and compared in Fig. 6(b). For both cases, 0℃ isotherms were located at a depth of 1 m below the ground surface. The internal temperature increased from −20℃ at the top boundary to 3℃ at the bottom boundary. The distance intervals between the isotherms were doubled from the 0℃ to 4℃ isotherms. While slight differences were observed along the horizontal direction, the overall agreement was reasonably close.

4. Freezing and thawing effects on retaining wall and backfill

4.1 Thermal distribution within backfill

From the thermal FE analyses described previously, the thermal distributions within the retaining wall and backfill were obtained for different T_a and GWL conditions. 0℃ isotherm, as freezing front, indicates the location of the interface between the unfrozen and frozen zones. Fig. 7 shows the 0℃ isotherm profiles within backfill for freezing durations from 1 to 90 days, GWLs at 0 and 2 m, and T_a equal to −10°C. Note that the 0℃ isotherms in Fig. 7 represent the freezing front and its propagation with time. Saturated zones above and below the 0℃ isotherm curves indicate the frozen and unfrozen zones, respectively. For the case with GWL = 0 m in Fig. 7(a), the frozen zone propagated along the wall down to a depth of 2.5 m after 30

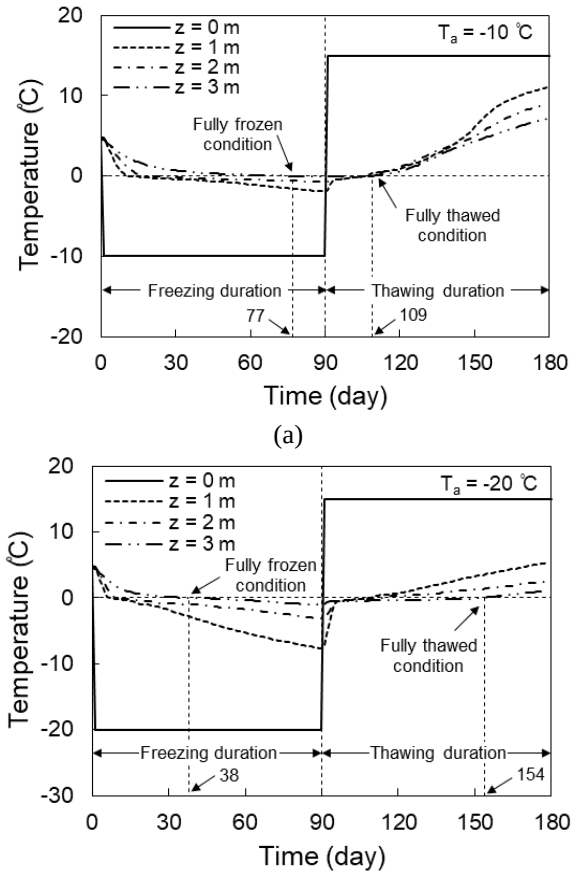

Fig. 8 Temperature variation with time at interface between retaining wall and backfill for T_a of (a) -10℃ and (b) -20℃

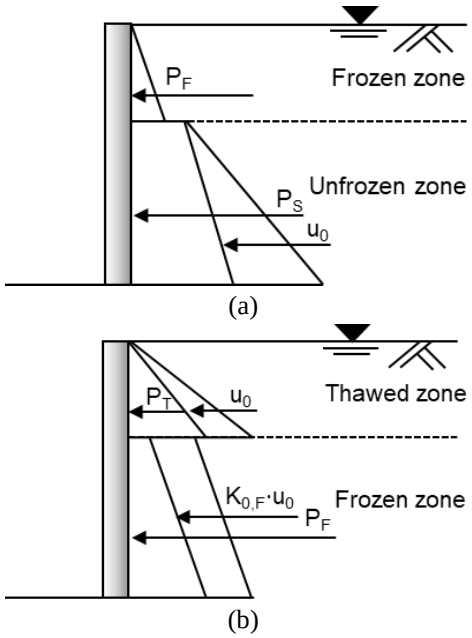

Fig. 9 Schematic distribution of lateral earth pressures at-rest: (a) freezing duration and (b) thawing duration

days and reached the bottom of the wall after 60 days. For the case with GWL = 2 m in Fig. 7(b), the frozen zone reached the depth of 2.6 m after 30 days and the bottom after 60 days. This indicates that the thermal propagation rates along the wall were quite similar for both GWL = 0 and 2 m. The thermal propagation within the internal soil zone, however, was much faster for GWL = 2 m, showing wider 0℃ isotherm intervals for the same freezing durations. This is because the dry soil zone exists above GWL that requires no phase change and thus no latent heat.

Fig. 8 shows the temperature variations with time for the soil along the retaining wall at different depths (z) with GWL = 0 m, compared for T_a = −10℃ and −20℃. The depths of z = 0 and 3 m correspond to the top and bottom of the backfill, respectively. For T_a = −10℃, a fully frozen condition was achieved throughout the entire backfill zone after 77 days while a fully thawed condition was reached after a thawing duration of 19 days. For T_a = −20℃, the fully frozen condition was achieved after 38 days, which is 39 days faster than for T_a = −10℃. A longer duration of 64 days was however required to reach the fully thawed condition. For GWL = 2 m, the temperature variation within the dry soil zone did not show a time delay for the phase change while the variation within the saturated soil zone was similar to that in Fig. 8 for GWL = 0 m.

4.2 Variation of at-rest lateral earth pressure

The mechanical FE analyses were performed in sequence, interactively with the results from the thermal FE analyses, to obtain changes in the mechanical state of the wall and backfill during freezing and thawing. Different values of K_0, as discussed in Fig. 3, were adopted into the unfrozen, frozen, and thawed zones identified from the thermal analyses. During freezing, the freezing front moves downward demonstrating an enlarged frozen zone and the lateral earth pressure acting on the wall decreases while the hydrostatic pore pressure (u_0) acts only within the unfrozen zone below the freezing front. This is described in Fig. 9(a). Note that P_F indicates the lateral earth pressure within the frozen soil zone where no hydrostatic pore pressure applies, and P_S represents the lateral earth pressure for the unfrozen soil condition. During thawing, the lateral earth pressure (P_T) increases as the thawing progresses and the hydrostatic pore pressure (u_0) becomes active for the thawed zone as shown in Fig. 9(b). Note that $K_{0,F}$ means the coefficient of the at-rest lateral earth pressure for the frozen condition. The total lateral earth pressure is then larger within the upper thawed zone than within the lower frozen zone. All these indicate that the lateral pressure acting on the wall and the location of the load application change during freezing and thawing, which would affect the overall stability of the retaining wall.

Fig. 10 shows the variations of the resultant lateral force at rest (P_0) acting on the wall during freezing and thawing, normalized with the initial unfrozen lateral force ($P_{0,ini}$) for different T_a and GWL conditions. Note that P_0 in Fig. 10 represents the total force including the pore-water force, which is another important component affecting the stability of the wall. It is clearly observed that P_0 decreases during freezing and increases after thawing. As shown in Fig. 10(a), for GWL = 2 m, P_0 decreased by 55% during

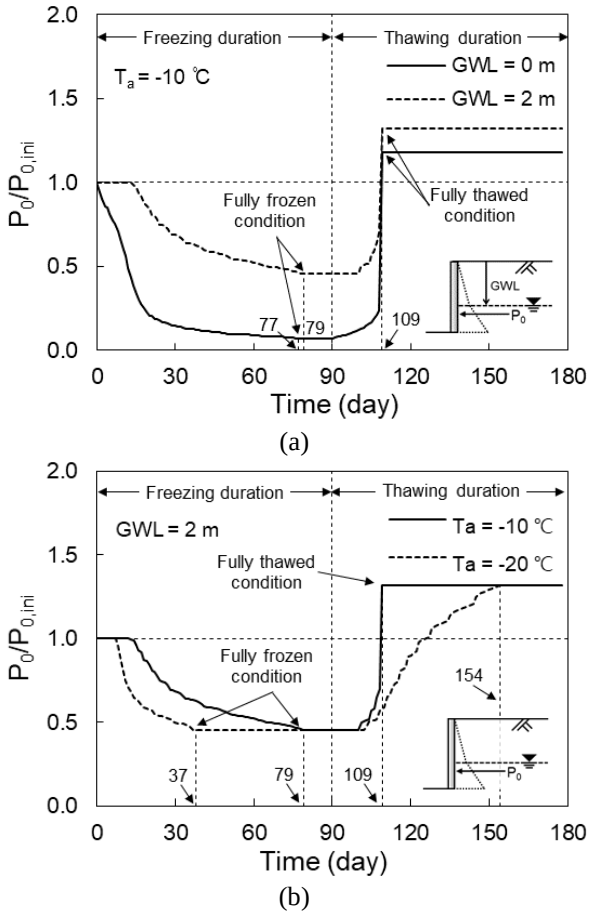

Fig. 10 Variation of $P_0/P_{0,ini}$ during freezing and thawing for different (a) GWLs and (b) T_as

freezing and eventually increased by 32% after thawing. For GWL = 0 m, P_0 decreased and increased by 93% and 18%, respectively, during freezing and thawing, which were higher and lower than for GWL = 2 m. This indicates that, even if backfill is not fully saturated, increases in P_0 due to freezing and thawing can be quite considerable, and should be properly addressed to consider the long-term and seasonal variation of wall stability.

As shown in Fig. 10(b), T_a controls the time required to reach the frozen and thawed conditions, while not affecting the magnitude of P_0. Note that the effect of capillary engagement during phase change was not considered in this study and thus the insensitiveness of P_0 to temperature shown in Fig. 10(b) may be limitedly valid only for such condition.

The time delays to reach the full mobilization of P_0 during thawing should also be addressed. It was due to the time required for heat transfer and phase change in soil toward thawed condition, similar to the distribution of freezing front in Fig. 7. As shown in Fig. 10(b), the time delays were the same for different GWLs at given T_a. For T_a of -10°C, the time delay was 19 days and longer time delay was observed for lower T_a of -20°C. This was because the lower part of backfill with groundwater was affected by the thermal conduction from the retaining wall rather than that from the backfill surface.

4.3 Mobilized overturning moment

During the freezing-thawing process, the application point of the resultant force acting on the retaining wall changes due to the changes of frozen zone. Fig. 11 shows the height (h) of the load application point, normalized by wall height (H), during freezing and thawing for different GWL [Fig. 11(a)] and T_a [Fig. 11(b)] conditions. For GWL = 0 m in Fig. 11(a), h/H decreased initially during freezing and then increased finally returning to the initial value after the fully frozen condition was reached. The initial decrease in h/H can be attributed to the partial frozen state with local decreases in lateral earth pressure before reaching the fully frozen condition after 77 days. During thawing, h/H increased until the 18th day after thawing was initiated and dropped for 1 day after the fully thawed condition was reached as the thawed zone became enlarged from the ground surface. For GWL = 2 m, the opposite trends of variations were observed. h/H gradually increased during freezing and decreased during thawing. It is noted that K_0 is not affected by the freezing and thawing within the upper dry-soil zone, whereas it changes within the lower saturated-soil zone below GWL. The effect of T_a is shown in Fig. 11(b). For T_as of both −10°C and −20°C, similar variations in h/H were observed. Differences were observed in elapsed time, which can be explained by the rate of internal temperature change of the backfill as presented in Fig. 8.

Key component of the stability of the retaining walls is the mobilized overturning moment (M_o) exerted by the lateral force acting on the wall. The values of M_o were obtained using the resultant lateral force and its application point given in Figs. 10 and 11. Fig. 12 shows the variations of M_o during freezing and thawing for different GWL and T_a conditions. In Fig. 12, M_o was normalized by the initial unfrozen moment ($M_{o,ini}$). As shown in Fig. 12(a), the effect of GWL on M_o was significant. During freezing, $M_o/M_{o,ini}$ decreased by around 7% and 74% for GWLs of 0 and 2 m, respectively. After the fully thawed condition was reached, M_o increased and eventually became 18% and 17% higher than $M_{o,ini}$ for GWL = 0 and 2 m, respectively. Fig. 12(b) shows the effect of T_a on M_o. It is observed that the magnitude of M_o is independent on T_a, whereas elapsed time to reach the minimum and maximum M_o during freezing and thawing appear to be different. A lower T_a resulted in a longer elapsed time to reach maximum M_o due to larger frozen zone within backfill.

The effects of GWL on the change of M_o were analyzed as shown in Fig. 12. The overturning moment (M_{ow}) due to the hydrostatic pore pressure with GWL was expressed as a normalized term of $M_{ow}/M_{o,ini}$. The values of $M_{ow}/M_{o,ini}$ for GWL = 0 and 2 m decreased from 0.75 and 0.06 to 0 during freezing duration as the saturated soil was frozen. The values of $M_{ow}/M_{o,ini}$ increased and returned to the original magnitudes due to u_0 through the thawing process. While the proportions of M_{ow} varied depending on the GWL conditions, the changes showed a rapid pattern similar to those of M_o. Overall increases in M_o after thawing were attributed to changes in the lateral effective stress of soil. As indicated previously, the effects of freezing and thawing

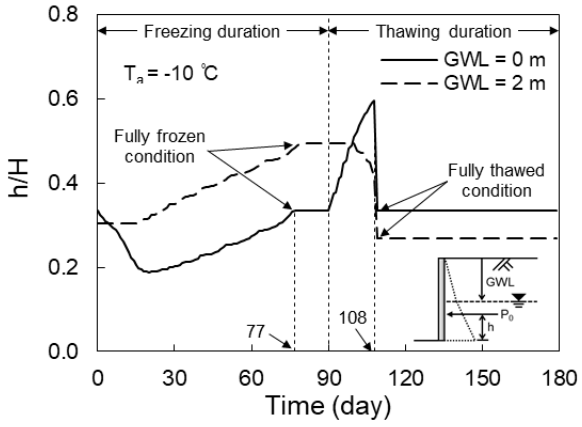

(a)

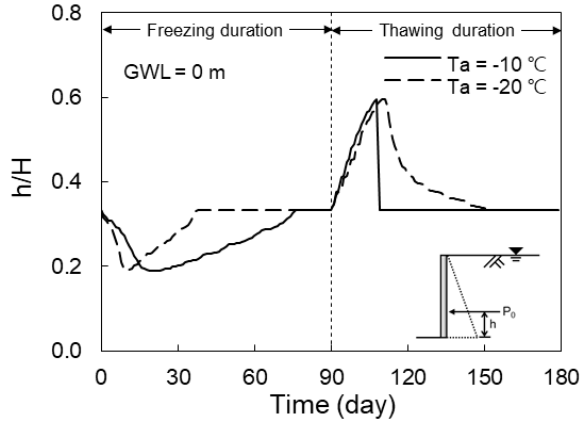

(b)

Fig. 11 Variation of h/H during freezing and thawing for different (a) GWLs and (b) T_as

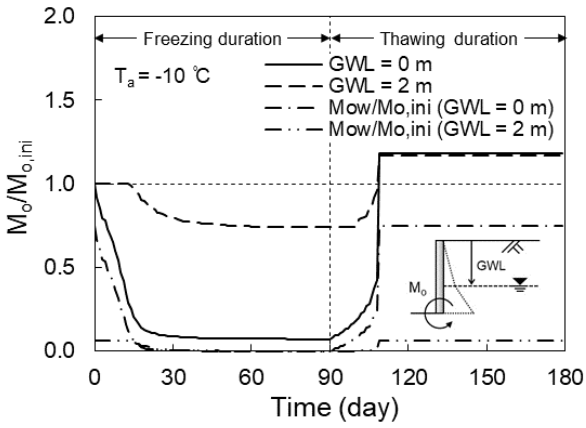

(a)

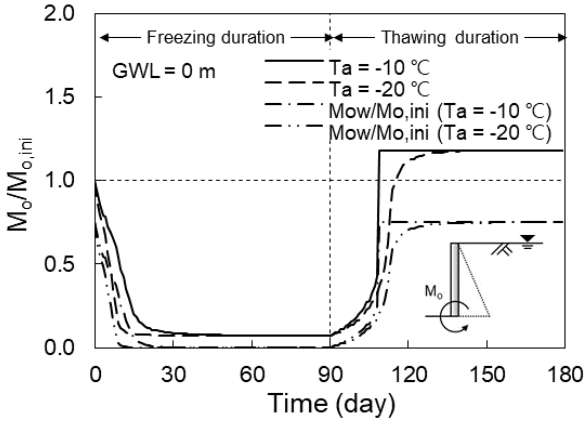

(b)

Fig. 12 Variation of $M_o/M_{o,ini}$ for different (a) GWL and (b) T_a conditions

shown in Figs. 10-12 were obtained for the condition without the consideration of capillary engagement during the phase change of water.

In summary, key findings and design implications obtained from Figs. 10-12 can be summarized as follows: (1) GWL affects significantly the changes in the lateral earth pressure and overturning moment acting on the wall during freezing and thawing; (2) T_a controls the elapsed time required for the variation of the lateral earth pressure and overturning moment; and (3) the mobilized overturning moment and wall stability during freezing and thawing vary in a pattern with abrupt change rather than gradual variation as indicated by the elapsed time to reach the fully frozen and thawed conditions. All these are important design considerations, implying that the reduction of safety margin and consequent wall collapse due to freezing and thawing can occur in sudden, unexpected patterns without any noticeable sign or other indication of failure.

4.4 Active and passive conditions

When the retaining wall moves away from or toward the backfill, the backfill reaches a plastic equilibrium condition, which is designated by the active and passive stress states as given by the coefficients of active and passive lateral earth pressures K_a and K_p, respectively. The values of K_a and K_p can be obtained by the following simple equations of Rankine's theory.

$$K_a = \frac{1-\sin\phi'}{1+\sin\phi'} \tag{3}$$

$$K_p = \frac{1+\sin\phi'}{1-\sin\phi'} \tag{4}$$

where ϕ' = internal friction angle.

For unfrozen soil, the mobilization of the lateral earth pressure with displacement has been studied extensively. According to Clough and Duncan (1991), the lateral wall displacements (δ) to reach the fully mobilized active state are 0.001H, 0.002H, and 0.004H for dense, medium dense, and loose sands, respectively. The lateral displacement for the passive state is about ten times larger than for the active state.

To investigate the effect of freezing and thawing on the active and passive stress states, additional thermal and mechanical FE analyses were performed. The active and passive stress states were induced by imposing wall rotation about the wall base for the unfrozen and fully thawed conditions. For the active case, the variations of K_a with wall displacement obtained from the FE analyses are shown in Fig. 13(a) for the unfrozen and thawed conditions. The

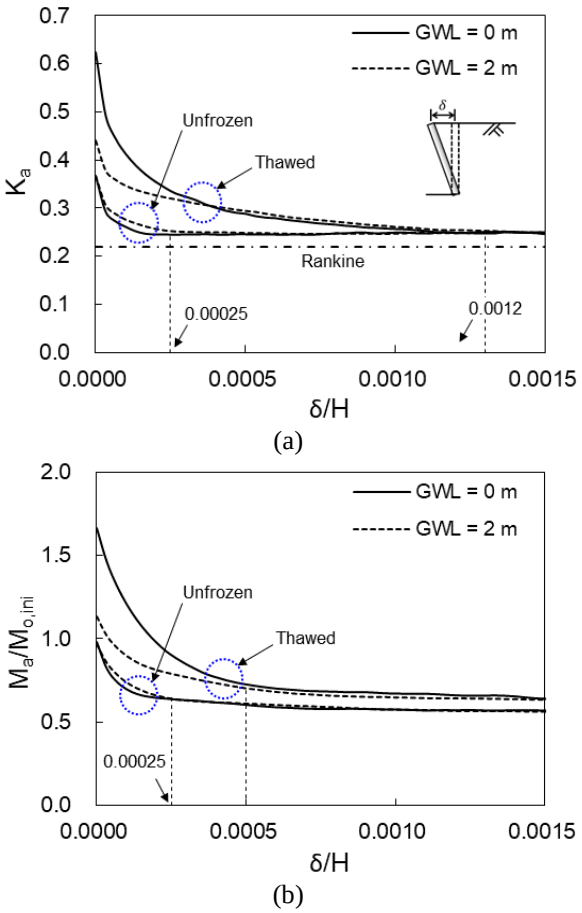

Fig. 13 Effect of freezing and thawing on active stress state: (a) K_a and (b) $M_a/M_{o,ini}$

values and variations of K_a were different for the unfrozen and thawed conditions. The lateral displacement to reach a fully mobilized active stress state was 0.0012H for the thawed condition, which was larger than 0.00025H for the unfrozen condition. The converged values of K_a for both cases were 0.25, which is slightly higher than 0.219 by Eq. (3) of the Rankine approach. The difference can be attributed to the partial mobilization of the active stress along the wall while the Rankine approach assumes a fully mobilized condition.

Fig. 13(b) shows changes in the normalized overturning moment ($M_a/M_{o,ini}$) for the active state with wall displacement. $M_a/M_{o,ini}$ decreased due to decreasing K_a shown in Fig. 13(a). As failure progressed with wall displacement, the values of $M_a/M_{o,ini}$ became nearly constant after δ/H of 0.00025 and 0.0005 for the unfrozen and thawed conditions, respectively. The converged values of $M_a/M_{o,ini}$ for the thawed condition were 1.2 times larger than for the unfrozen condition.

The variations in K_p and $M_p/M_{o,ini}$ for the passive state are given in Figs. 14(a) and 14(b), respectively. The differences in both K_p and $M_p/M_{o,ini}$ between the unfrozen and thawed conditions were not significant. This is because the mobilized passive earth pressure is 15 to 20 times larger than the at-rest lateral earth pressure, and the difference due to freezing and thawing is relatively small. This also indicates that the effect of freezing and thawing may not be an issue for retaining walls with the passive condition, while certain consideration is necessary for the at-rest and active conditions.

5. Effect of temperature fluctuation and wall insulation

The atmospheric temperature fluctuates with some periodicity. As the thermal FE analyses in this study were based on a constant average T_a, the effect of temperature fluctuation on the thermal distribution within backfill was checked and compared with that using an average T_a. Fig. 15(a) shows three cases of T_a variation with time, which were adopted in the additional thermal FE analyses. Case 1 represents a constant T_a, as in the previous analyses, and cases 2 and 3 indicate cyclic variations of T_a with different periods. As shown in Fig. 15(b), the thermal distributions of the freezing front with a 0℃ isotherm were all similar regardless of the number of cycles and time variation of T_a. Similar to the case of constant temperature condition, the results in Fig. 15(b) were obtained for the condition without considering the water capillary migration and consequent mechanical results would be limitedly valid only for such condition.

Insulation layer between the retaining wall and the backfill is an effective option to reduce the heat conduction from the wall face and hence the effect of freezing and

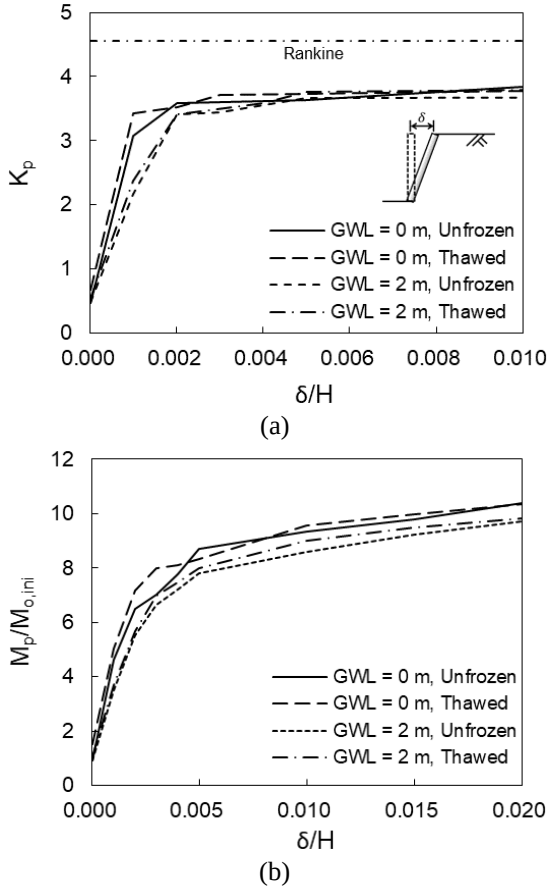

Fig. 14 Effect of freezing and thawing on passive stress state: (a) K_p and (b) $M_p/M_{o,ini}$

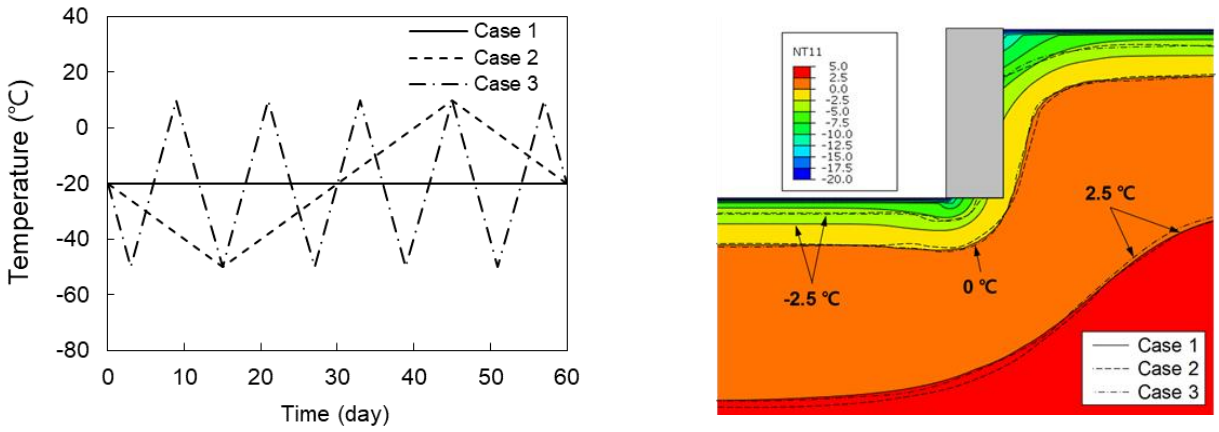

(a) (b)

Fig. 15 Comparison of temperature profile conditions: (a) time variation of T_a and (b) temperature distribution for different T_a profiles

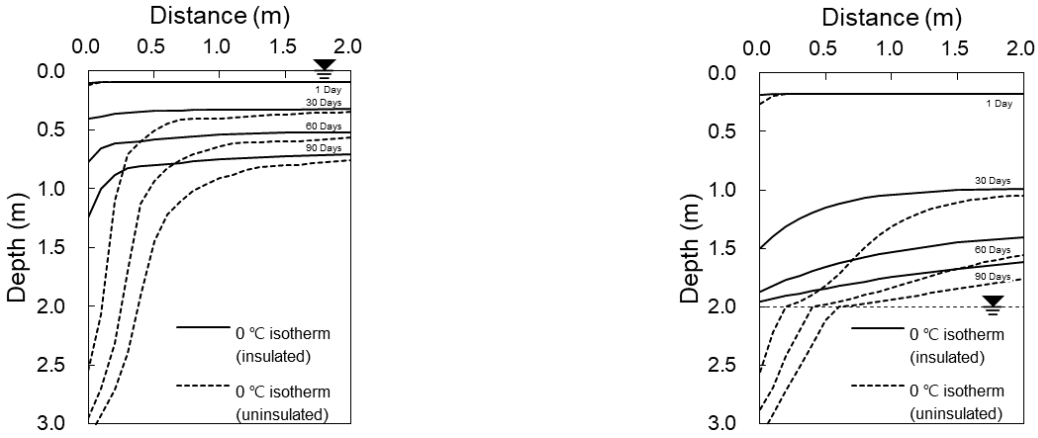

(a) (b)

Fig. 16 Comparison of insulated and uninsulated cases for (a) GWL = 0 m and (b) GWL = 2 m

thawing (Michałowski and Zhu 2006, Zhang 2014). To check the efficiency of the insulation layer, a retaining wall with an insulation layer was modeled and used in the thermal FE analysis. In the FE analyses, an insulation layer with the thickness of 0.1 m was considered as placed along the wall facing. The thermal conductivity and specific heat capacity of the insulation layer were 0.03 W/m·K and 2000 J/kg·K, respectively, based on the properties given by Michałowski and Zhu (2006).

Fig. 16 shows the 0℃ isotherm profiles within backfill with T_a = −10℃ and GWL = 0 and 2 m, compared for the insulated and uninsulated cases. Note that the zones above the 0℃ isotherm curves indicate frozen zones. For GWL = 0 m in Fig. 16(a), the propagation of the freezing front was delayed when the wall facing was insulated, compared to the uninsulated case. When insulated, the freezing front along the wall did not reach the half depth of the backfill during the 90 days freezing time, whereas two thirds of the backfill were already frozen for the uninsulated case. For GWL = 2 m in Fig. 16(b), a similar propagation delay was observed whereas the temperature propagation within backfill was much faster due to the existence of dry zone. The frozen zone was not observed with insulation even for 90 days. These results show that the use of insulation layer can be effective and beneficial for reducing or delaying the reduction in the safety margin due to the freezing-thawing process. It also indicates the effects of preventing the freezing and thawing of backfill and the clogging of drainage holes filled with frozen materials.

6. Conclusions

In this study, the effects of freezing and thawing on the mechanical behavior and stability of retaining wall were investigated for various temperature and groundwater level (GWL) conditions. For this purpose, the thermal and mechanical FE analyses were performed. Different freezing temperatures of −10°C and −20℃ and GWLs of 0 and 2 m within backfill were considered in the analyses. The external temperature (T_a) controlled the time required to reach the frozen and thawed conditions of backfill while not affecting the resultant lateral force at rest (P_0). GWL affected significantly P_0 and overturning moment (M_o) acting on the wall during freezing and thawing.

The thermal propagation within the saturated soil zone

along the wall was quite similar for both GWL = 0 and 2 m. The thermal propagation increased the P_0 acting on the wall after thawing for all conditions. This indicates that, even if the backfill is not fully saturated, increases in P_0 due to freezing and thawing can be quite considerable, and should be properly addressed for the long-term, seasonal variation of wall stability. The variation of mobilized M_o and wall stability with time indicated a pattern with abrupt change rather than gradual variation, implying that the reduction of safety margin and wall collapse due to freezing and thawing can occur in sudden, unexpected pattern. The effect of freezing and thawing was not significant for the passive case while some increase in the M_o was observed for the active case.

The effect of insulation layer between the retaining wall and the backfill was positively noticeable. It was quite effective for reducing the heat conduction from wall, and hence, for reducing the freezing- and thawing-induced changes in the safety margin. In addition, further studies can be followed to address the condition of more realistic wall shape as the current study was based on a simplified wall configuration.

Acknowledgments

This work was supported by the National Research Foundation of Korea (NRF), the Korea Institute of Energy Technology Evaluation and Planning (KETEP) and the Ministry of Trade, Industry and Energy (MOTIE), with grants funded by the government of Korea (Project Nos. 20194030202460 and 2020R1A2C2011966). It was also supported by the Korea Agency for Infrastructure Technology Advancement (KAIA) grant funded by the Ministry of Land, Infrastructure and Transport (National Research for Smart Construction Technology, No. 20SMIP-A158708-01).

References

Andersland, O.B. and Anderson, D.M. (1978), *Geotechnical Engineering for Cold Regions*, McGraw-Hill, New York, U.S.A.

Andersland, O.B. and Ladanyi, B. (2004), *Frozen Ground Engineering*, (2nd Edition), American Society of Civil Engineering, John Wiley and Sons, Hoboken, New Jersey, U.S.A.

Babaei, M. (2016), "Finite element analysis of freezing effect on soil nail wall", Ph.D. Dissertation, Ryerson University, Toronto, Canada.

Bentler, J. and Labuz, J. (2006), "Performance of a cantilever retaining wall", *J. Geotech. Geoenviron. Eng.*, **132**(8), 1062-1070. https://doi.org/10.1061/(ASCE)1090-0241(2006)132:8(1062).

Blake, J.R., Renaud, J.P., Anderson, M.G. and Hencher, S.R. (2003), "Prediction of rainfall-induced transient water pressure head behind a retaining wall using a high-resolution finite element model", *Comput. Geotech.*, **30**(6), 431-442. https://doi.org/10.1016/S0266-352X(03)00055-7.

Brooker, E.W. and Ireland, H.O. (1965), "Earth pressures at rest related to stress history", *Can. Geotech. J.*, **2**(1), 1-15. https://doi.org/10.1139/t65-001.

Chamberlain, E.J. and Gow, A.J. (1979), "Effect of freezing and thawing on the permeability and structure of soils", *Eng. Geol.*, **13**(1-4), 73-92. https://doi.org/10.1016/0013-7952(79)90022-X.

Clough, G.W. and Duncan, J.M. (1971), "Finite element analyses of retaining wall behavior", *J. Soil. Mech. Found. Div.*, **97**(12), 1657-1673.

Côté, J. and Konrad, J.M. (2005), "A generalized thermal conductivity model for soils and construction materials", *Can. Geotech. J.*, **42**(2), 443-458. https://doi.org/10.1139/t04-106.

Eigenbrod, K.D. (1996), "Effects of cyclic freezing and thawing on volume changes and permeabilities of soft fine-gained soils", *Can. Geotech. J.*, **33**(4), 529-537. https://doi.org/10.1139/t96-079-301.

Farouki, O.T. (1981), "Thermal properties of soil in cold regions", *Cold Reg. Sci. Technol.*, **5**(1), 67-75. https://doi.org/10.1016/0165-232X(81)90041-0.

Graham, J. and Au, V.C.S. (1985), "Effects of freeze-thaw and softening on a natural clay at low stresses", *Can. Geotech. J.*, **22**(1), 69-78. https://doi.org/10.1139/t85-007.

Jame, Y.W. and Norum, D.I. (1980), "Heat and mass transfer in a freezing unsaturated porous medium", *Water Resour. Res.* **16**(4), 811-819. https://doi.org/10.1029/WR016i004p00811.

Jin, H.W., Lee, J., Ryu, B.H., Shin, Y. and Jang, Y. (2019), "Experimental assessment of the effect of frozen fringe thickness on frost heave", *Geomech. Eng.*, **19**(2), 193-199. http://doi.org/10.12989/gae.2019.19.2.193.

Kim, I., Lee, D., Kim, Y., Yun, T.S. and Lee, J. (2021), "Effects of pore water volume on K_0 for sand subject to freezing and thawing", *J. Geotech. Geoenviron. Eng.*, **147**(3), 04020173. https://doi.org/10.1061/(ASCE)GT.1943-5606.0002468.

Lee, S. (2019), "Experimental study on effect of underground excavation distance on the behavior of retaining wall", *Geomech. Eng.*, **17**(5), 413-420. http://doi.org/10.12989/gae.2019.17.5.413.

Lee, J., Lee, D., Park, D., Kyung, D., Kim, G. and Kim, I. (2016), "Effect of freezing and thawing on K_0 geostatic state for granular materials", *Granul. Matter.* **18**, 69. https://doi.org/10.1007/s10035-016-0665-6.

Leroueil, S., Tardif, J., Roy, M., Rochelle, P.L. and Konrad, J.M. (1991), "Effects of frost on the mechanical behaviour of Champlain Sea clays", *Can. Geotech. J.*, **28**(5), 690-697. https://doi.org/10.1139/t91-083.

Liu, J., Chang, D. and Yu, Q. (2016), "Influence of freeze-thaw cycles on mechanical properties of a silty sand", *Eng. Geol.*, **210**, 23-32. https://doi.org/10.1016/j.enggeo.2016.05.019.

Michałowski, R.L. and Zhu, M. (2006), "Modelling of freezing in frost-susceptible soils", *Comput. Assisted Mech. Eng. Sci.*, **13**, 613-625.

Milly, P.C.D. (1984), "A simulation analysis of thermal effects on evaporation from soil", *Water Resour. Res.*, **20**(8), 1087-1098. https://doi.org/10.1029/WR020i008p01087.

Paudel, B. and Wang, B. (2010), "Freeze-thaw effect on consolidation of the soils from the Mackenzie valley, Canada", *Proceedings of the Geo2010 - the 63rd Canadian Geotechnical Conference and 1st Joint CGS/CNC-IPA Permafrost Specialty Conference*, Calgary, Canada, September.

Qi, J., Vermeer, P.A. and Cheng, G. (2006), "A review of the influence of freeze-thaw cycles on soil geotechnical properties", *Permafrost Periglac.*, **17**(3), 245-252. https://doi.org/10.1002/ppp.559.

Saggu, R. and Chakraborty, T. (2017), "Thermomechanical analysis and parametric study of geothermal energy piles in sand", *Int. J. Geomech.*, **17**(9), 04017076. https://doi.org/10.1061/(ASCE)GM.1943-5622.0000962.

Tang, L., Du, Y., Liu, L., Jin, L., Yang, L. and Li, G. (2020), "Effect mechanism of unfrozen water on the frozen soil-structure interface during the freezing-thawing process",

Geomech. Eng., **22**(3), 245-254. http://doi.org/10.12989/gae.2020.22.3.245.

Wang, D.Y., Ma, W., Niu, Y.H., Chang, X.X. and Wen, Z. (2007), "Effects of cyclic freezing and thawing on mechanical properties of Qinghai–Tibet clay", *Cold Reg. Sci. Technol.*, **48**(1), 34-43. https://doi.org/10.1016/j.coldregions.2006.09.008.

Yao, X., Qi, J. and Yu, F. (2014), "Study on lateral earth pressure coefficient at rest for frozen soils", *J. Offshore Mech. Arct. Eng.*, **136**(1), 011301. https://doi.org/10.1115/1.4025546.

Yoo, C. and Jung, H. (2006), "Case history of geosynthetic reinforced segmental retaining wall failure", *J. Geotech. Geoenviron. Eng.*, **132**(12), 1538-1548. https://doi.org/10.1061/(ASCE)1090-0241(2006)132:12(1538).

Yun, T.S. and Santamarina, J.C. (2008), "Fundamental study of thermal conduction in dry soils", *Granul. Matter.*, **10**(3), 197-207. https://doi.org/10.1007/s10035-007-0051-5.

Zhang, L., Ma, W., Yang, C. and Yuan, C. (2014), "Investigation of the pore water pressures of coarse-grained sandy soil during open-system step-freezing and thawing tests", *Eng. Geol.* **181**, 233-248. https://doi.org/10.1016/j.enggeo.2014.07.020.

Zhang, Y. (2014), "Thermal-hydro-mechanical model for freezing and thawing of soils", Ph.D Dissertation, University of Michigan, Michigan, U.S.A.

CC